physics

MDPI

Article

Recent Achievements in NAA, PAA, XRF, IBA and AMS Applications for Cultural Heritage Investigations at Nuclear Physics Institute, Řež

Jan Kučera *, Jan Kameník, Vladimír Havránek, Ivana Krausová, Ivo Světlík, Kateřina Pachnerová Brabcová, Marek Fikrle and David Chvátil

Nuclear Physics Institute of the Czech Academy of Sciences, 250 68 Husinec-Řež, Czech Republic; kamenik@ujf.cas.cz (J.K.); havranek@ujf.cas.cz (V.H.); krausova@ujf.cas.cz (I.K.); svetlik@ujf.cas.cz (I.S.); brabcova@ujf.cas.cz (K.P.B.); fikrle@ujf.cas.cz (M.F.); chvatil@ujf.cas.cz (D.C.)
* Correspondence: kucera@ujf.cas.cz

Abstract: Five case studies are reported on the use of neutron and photon activation analysis (NAA and PAA, respectively), X-ray fluorescence (XRF) analysis, ion beam analysis (IBA), and accelerator mass spectrometry (AMS) for the elemental characterization or dating of various objects of cultural heritage, such as building materials, pottery, metallic artefacts, ancient decorations, or the remains of historical personalities. The use of the individual techniques or their combination proved a useful, frequently indispensable tool for revealing the provenance of the artefacts, the method and time of their manufacturing, the elucidation of ancient human activities, or the verification of various hypotheses or legends related to the artefacts.

Keywords: neutron activation analysis; photon activation analysis; X-ray fluorescence analysis; ion beam analysis; accelerator mass spectrometry; cultural heritage

check for updates

Citation: Kučera, J.; Kameník, J.; Havránek, V.; Krausová, I.; Světlík, I.; Pachnerová Brabcová, K.; Fikrle, M.; Chvátil, D. Recent Achievements in NAA, PAA, XRF, IBA and AMS Applications for Cultural Heritage Investigations at Nuclear Physics Institute, Řež. *Physics* **2022**, *4*, 491–503. https://doi.org/10.3390/physics4020033

Received: 24 January 2022
Accepted: 4 April 2022
Published: 28 April 2022

Publisher's Note: MDPI stays neutral with regard to jurisdictional claims in published maps and institutional affiliations.

Copyright: © 2022 by the authors. Licensee MDPI, Basel, Switzerland. This article is an open access article distributed under the terms and conditions of the Creative Commons Attribution (CC BY) license (https://creativecommons.org/licenses/by/4.0/).

1. Introduction

Non-destructive and non-invasive methods are of significant importance for cultural heritage investigation. Nuclear physics offers a wide array of principles and techniques, which can be utilized for the above purpose. They encompass interactions of matter with neutron and ion beams, and other types of ionizing radiation. Due to the enormous progress of these technologies in recent decades, they offer multi-elemental or multi-species determination with very low detection limits, frequently with a good spatial resolution. Therefore, they find increasing use in the characterization of cultural heritage objects that help us to understand the way of life and achievements of ancient civilizations. A topical review [1] gives an account of ion beam analysis (IBA), neutron beam analytical methods, dating methods, such as luminescence dating and accelerator mass spectrometry (AMS), and complimentary methods, such as γ-beam techniques, X-ray fluorescence (XRF), and nuclear magnetic resonance (NMR), and provides numerous examples of applications of these techniques in cultural heritage research and preservation. A brief summary of some of the above techniques and their applications is also given in another review [2]. A recent book [3] gives an overview of the main spectroscopy and diffraction techniques, namely Raman and infrared spectroscopy, spectroscopy and diffraction using an electron microscope, UV(ultraviolet)–visible–near–IR(infrared) reflectance spectrophotometry, neutron and X-ray tomography, X-ray and neutron diffraction, laser-induced breakdown spectroscopy, laboratory and synchrotron X-ray spectroscopy, IBA, and high-energy particle analysis, with comments on combining and comparing multiple techniques, sources of error, and the limitations of the analytical methods currently available for cultural heritage research. IBA techniques, including Rutherford backscattering spectrometry, elastic recoil detection, non-Rutherford elastic backscattering, nuclear reaction analysis, particle-induced

gamma-ray emission, and particle-induced X-ray emission, are explained, with particular emphasis on thin-film analysis in a review by Jeynes and Colaux [4].

Cultural heritage studies have been pursued at the Nuclear Physics Institute (NPI) of the Czech Academy of Sciences (CAS) using nuclear and related analytical techniques, such as neutron and photon activation analysis, XRF analysis, IBA, and radiocarbon dating with accelerator mass spectrometry, by taking advantage of suitable experimental facilities available for these purposes. The facilities available are briefly described and examples of recent achievements, employing the individual techniques or their combinations, are presented in this work.

2. Experimental

2.1. Neutron Activation Analysis (NAA)

Neutron irradiation is carried out at a light-water tank-type research nuclear reactor LVR-15 operated by Research Centre Řež. The reactor has a maximal thermal power of 10 MW and a maximal thermal neutron flux in the reactor core of $1{\cdot}10^{14}$ cm^{-2} s^{-1} [5]. For short-time irradiation (10 s–3 min), a vertical channel in the corner of the active core equipped with a pneumatic transport system is used to deliver samples in polyethylene (PE) rabbits to the laboratory within 3.5 s. For long-time irradiation (several hours to several days) in Al cans, three vertical channels located in a Be reflector at the outskirts of the active core can be used. The maximum neutron fluxes available in these channels amount to $3.1–7.0{\cdot}10^{13}$ cm^{-2} s^{-1}, $8.4{\cdot}10^{12}$ cm^{-2} s^{-1}–$1.0{\cdot}10^{13}$ cm^{-2} s^{-1}, and $5.6{\cdot}10^{12}$ cm^{-2} s^{-1} –$6.4{\cdot}10^{13}$ cm^{-2} s^{-1} for thermal, epithermal and fast neutrons, respectively. Selective irradiation with epithermal and fast neutrons can be realized using special capsules made of or inlaid with 1 mm-thick Cd shielding. Short-time irradiation is carried out with individual samples and calibrators together with neutron fluence monitors. Long-time irradiation is performed batch-wise, with 20–25 samples, calibrators and neutron flux monitors in each batch.

Samples with a mass in the range of several mg to several hundred mg are heat-sealed for irradiation lasting from 10 s to 5 h into PE disk-shaped capsules with a diameter of 25 mm prepared by sealing two acid-cleaned PE disks with a thickness of 0.15 mm. For longer irradiation times over several hours, samples are to be sealed into ampoules made of high-purity quartz glass. Specific sample preparation procedures are described in the corresponding sections. For gamma-ray spectrometry measurements of the induced radionuclides, several high-purity germanium detectors (HPGe) with a relative efficiency of 21–78% and FWHM (full width at half maximum) resolution of 1.75 keV–1.85 keV (at the 1332.5 keV gamma-line of ^{60}Co) are available. The detectors are interfaced to a computer-controlled Genie 2000™ (Canberra) gamma-ray spectrometer.

For the quantification of element contents, either relative or k_0-standardization can be used. The former method is based on the irradiation of calibrators of elements to be determined simultaneously with the samples [6]. In the latter "standardless" method, the samples are irradiated with neutron flux monitors for the evaluation of neutron flux parameters, and for the quantification of element contents, k_0-factors are employed [7]. The preparation of calibrators and neutron fluence monitors for both procedures, as well as typical decay and counting times, have been described in detail elsewhere [6–9].

2.2. Photon Activation Analysis (PAA)

Irradiation with high-energy photons is carried out in a laboratory with microtron MT25, a cyclic accelerator of electrons, which move within a vacuum chamber in circular trajectories with gradually increasing diameters, thus gaining gradually higher energy. They can be extracted from individual orbits to achieve the required beam energy. Thus, electrons with the energy in the range 6–25 MeV can be obtained with the mean current of 30 μA at 23 MeV [10]. The accelerated electron beam is converted into high-energy photon radiation (Bremsstrahlung) by the bombardment of a water-cooled tungsten target. A photon flux has been calculated to amount, for instance, to $6{\cdot}10^{11}$ cm^{-2} s^{-1} at a 10 μA

beam current. A common procedure of sample, calibrator and photon fluence monitor preparation is as follows. Samples with a mass of several grams are usually sealed into PE disc-shaped capsules with a diameter of 35 mm. Calibrators are prepared by weighing pure elements or their stoichiometrically defined compounds, sometimes mixed with starch or cellulose powder to match the same geometry in the PE capsules as that for the samples. Copper foils with the same diameter as the samples and calibrators are used for monitoring the Bremsstrahlung photon fluence. Samples, calibrators and monitors are irradiated in a rotation device with 24 positions located several cm from the tungsten converter, so that the axis of rotation (2 rotations min^{-1}) is perpendicular to that of the beam. Other experimental details and radionuclides measured by gamma-ray spectrometry have already been given elsewhere [6].

In one of the presented case studies (cf. Section 3.3), there was a need to irradiate a whole voluminous specimen (an ancient bracelet with unknown matrix) with a diameter of 75 mm and a mass of 9.531 g to determine non-destructively nitrogen via the nuclear reaction $^{14}N(\gamma,n)^{13}N$, $T_{1/2}$ = 9.97 min. Therefore, the whole specimen was fixed in a PE bag rotated at a 10 cm distance from the converter (Figure 1), as well as studied "matrix" materials, and the calibrator made of 0.814 g of NH_4SCN mixed with starch in a shape matching those of the samples analysed.



Figure 1. Experimental set-up for Bremsstrahlung irradiation of the whole rotated bracelet (insert in lower right corner) in a microtron MT25 (according to [11]).

2.3. X-ray Fluorescence Analysis

The XRF laboratory of NPI is equipped with a benchtop SpectroMidex spectrometer (Figure 2) of the third generation with a Mo X-ray tube operated at 45 kV and 0.5 mA. The spectrometer has a programmable motorized sample support table, which together with four different square collimators with a side length of 0.1 mm, 0.3 mm, 0.5 mm and 2 mm, allow the production of surface 2-dimensional (2D) maps with a resolution of 0.1 mm for one point. The space between the sample and detector can be flushed with He, which together with a short sample-to-detector distance makes it possible to determine the elements ranging from Na to U. The spectrometer set-up is optimal for the analysis of coins, different types of metals and artefacts, but also fragments of glass, plasters or pigments on paintings.

The SpectroMidex has its own software for sample measurement and results evaluation, which can be modified according to the actual needs. The quantification is based on the so-called standard-based fundamental parameters method for thick samples. The preloaded procedures were optimized with the aid of numerous reference materials of copper alloys and the noble metals Au and Ag, with the composition matching well with that of the

historical specimens. In this way, more accurate results are obtained here for historical samples of coins and metal pieces, compared with the standard methods from the manufacturer. In this way, the quantification of the analysis of other specimen types can also be adapted.



Figure 2. X-ray fluorescence (XRF) spectrometer SpectroMidex (AMETEC, Kleve, Germany).

2.4. Ion Beam Analysis (IBA)

NPI maintains a compact, multipurpose linear electrostatic tandem accelerator Tandetron 4130 MC with an operating energy range of 200 keV–10 MeV, and a terminal voltage of 200 kV–3 MV, which produces accelerated ions from H to Au with ion beam currents in the range of nA to µA. Among other applications, the Tandetron accelerator can be used for various IBA techniques, namely Rutherford backscattering (RBS), which is a special case of elastic backscattering spectrometry (EBS) [12], RBS-channeling, elastic recoil detection analysis (ERDA), ERDA-time-of-flight, particle-induced X-ray emission (PIXE), particle-induced gamma-ray emission (PIGE), and ion-microprobe with less than 1 µm lateral resolution. The ion-microbeam system equipped with Oxford Instruments ion optics uses a chamber with a detector array for 3D elemental mapping, simultaneously using PIXE, PIGE, and RBS [13]. This device was employed in the present work for lead determination in single hairs of Tycho Brahe in one of the presented case studies (cf. Section 3.5) using a 2.6 MeV proton beam, focused to a diameter of 1.5 µm. Multiple scans were performed over 500 µm sections of hair at several distances from the hair bulb, using a 0.1 nA beam current for 1–3 h. The quantification was carried out using the GUPIX computer code [14] from Pb L-lines. Notably, the GUPIX code has recently been updated and expanded, with emphasis on the 1–15 keV X-ray energy range accessed by silicon drift detectors [15]. The detector was calibrated using a set of thick targets and the proton dose was determined from the EBS spectra using the "Q factor" method (the ratio between the true charge and the measured charge) [16]. Finally, the results were normalized against the sulfur content, with a reference value of 6.2 mass per cent.

2.5. Radiocarbon Dating Using Accelerator Mass Spectrometry

Key advances in ^{14}C measurement and instrumentation for radiocarbon dating, as well as optimal sample selection and preparation, were outlined in a recent review [17]. Radiocarbon dating is carried out in a laboratory under the international code CRL jointly operated by NPI and the Institute of Archaelogy of the CAS, Prague. The laboratory is equipped for the decay counting of ^{14}C by two low-background liquid scintillation counting spectrometers 1220 QUANTULUS™ (PerkinElmer, Shelton, CT, USA). However, in anticipation of the establishment of the first AMS laboratory in the Czech Republic equipped with a 300 kV AMS system MILEA, which was put into operation in 2022 [18], the graphitization of samples for AMS has already been mastered in the CRL laboratory. Samples prepared for AMS have so far been measured in a cooperating laboratory HEKAL ATOMKI HAS (Hungarian Academy of Sciences), Debrecen, using the MICADAS AMS system [19,20]. Samples of bones, wood, charcoal, and related materials are first pretreated

by relevant purification routines according to [21,22] and dried at 60 °C to a constant weight. The pretreated samples, together with a small amount of CuO (oxidation agent), are torch-sealed into partially evacuated quartz glass tubes and combusted at 900 °C for several hours. The resulting CO_2 is then purified and graphitized with Zn as a sole reducing agent [23,24]. The graphitized samples are sealed in vacuum and delivered for AMS measurement to the ATOMKI laboratory. For calibration, graphitized Secondary Oxalic Acid HOX II, the US National Institute of Standards and Technology (NIST) Standard Reference Material (SRM) NIST SRM® 4990 is used. Dating interpretation of analytical results is performed employing the OxCal software and the radiocarbon calibration curve IntCal 20 [25]. A somewhat modified sample pretreatment procedure was used for the dating of charcoal paintings, as described in Section 3.4 [26].

3. Case Studies

3.1. NAA of Sandstone from Khmer Temples, Cambodia

Magnificent Khmer temples at Angkor in Cambodia, included in the World Heritage list in 1992, were built in the period spanning from the 9th to 13th century, during the golden age of the Khmer empire. The chronology and architectural styles of the Angkor temples are known namely based on epigraphic and stylistic studies carried out by the École française d'Extrême-Orient (EFEO), Paris, since 1907 [27]. However, very little information is available about the petrology and the origin of the sandstone construction blocks from which the temples were mostly constructed. Several teams from France, Japan, China, the U.S., etc., are studying the origin of the Khmer temples and sandstone building materials, which are petrologically classified as feldspatic arenite, quartz arenite, and feldspatic to lithic wacke, under the auspices of APSARA (Autorite pour la Protection du Site et l'Amenagement de la Region d'Angkor). Magnetic susceptibility measurements revealed that several sandstone quarries of unknown location were used for the supply of building blocks [28]. To distinguish the three main sandstone types, non-destructive and in situ measurements using a portable magnetic susceptibility meter and a portable X-ray fluorescence analyser were also performed. The Rb, Sr and Y contents determined and magnetic susceptibility values demonstrated different sandstone source locations [29]. To extend existing knowledge about the elemental composition of sandstone, from which the individual temples were built, and its possible correlation with a building period (style) of a temple, instrumental NAA (INAA) is used by taking advantage of the technique's multi-elemental capability, low detection limits for many elements, inherent accuracy potential for bulk analysis when a representative sample aliquot can be prepared, and favourable experimental conditions, available at NPI.

Samples of sandstone were obtained from the building blocks of 19 individual temples and two presumed quarries by core drilling. Cores of up to 7 cm long were extracted with a diamond core drill bit with a diameter of 12 mm. Only the innermost part of the cores, 4 to 5 cm from the surface layer, was selected for the comparative elemental study to avoid the analysis of sandstone surface layers with a composition altered by weathering and other degradation process, such as lichen growths. Other details of sample preparation were published earlier [30]. For quality control (QC) purposes, reference materials of the US Geological Survey (USGS) AGV-1 (Andesite), the NIST SRM® 2704 (Buffalo River Sediment) and NIST SRM® 1633b (Coal Fly Ash) were used.

Using the INAA procedure with both short-time and long-time irradiation (1 min and 2 h, respectively), described earlier [6,11,31], the contents of 35 major, minor and trace elements, namely Na, Mg, Al, Si, K, Ca, Sc, Ti, V, Cr, Mn, Fe, Co, Zn, Rb, Sr, Zr, Sb, Cs, Ba, La, Ce, Nd, Sm, Eu, Gd, Tb, Dy, Tm, Yb, Lu, Hf, Ta, Th, and U are determined. The values obtained for QC samples proved validation of the procedure used. The average values for all 35 elements in the sandstone samples were examined with cluster analysis using Euclidean distance and average linkage to establish whether the sandstone elemental composition correlates with the construction period (and architectural style) of the individual temples. The cluster analysis dendrogram (Figure 3) showed that except for one

separate cluster for the sandstone of the Banteay Srei temple (built from red quartzose arenite), other clusters show only a partial correlation with the construction periods of the temples. A similar pattern was found when we examined by cluster analysis the major components, selected minor or trace elements, or mineralogical composition of the sandstone samples [30]. We suggested two possible reasons for the poor correlation between the sandstone chemical or mineralogical composition and the known construction period of the temples: (a) the inherent inhomogeneity of sandstone, which prevents the preparation of a representative test portion of about 150 mg from ~2 g of a homogenized sandstone analytical sample; and (b) the sandstone building blocks were taken from several (yet unknown) quarries during the construction of a particular temple or its part. The latter explanation, which was a novel one when our results were published in 2008 [30], was recently confirmed by a group of Japanese scientists in 2021 [29].

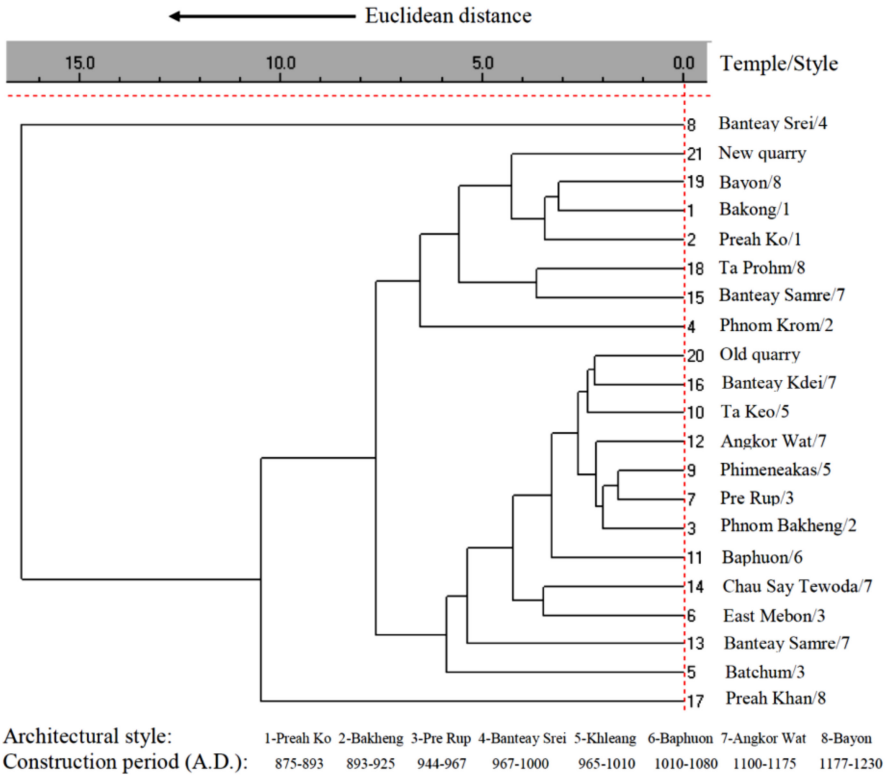

Figure 3. Dendrogram of sandstone elemental composition of Angkor temples (according to [30]).

3.2. XRF and INAA of Historical Coins and Ancient Metallic Artefacts

XRF is an optimal technique for the determination of major and minor elements in archaeological artefacts, frequently in metallic objects, due to the technique's advantageous features; it is fast, simple, and non-destructive in both sampling and analysis steps. On the other hand, XRF is a method with strong matrix effects, which is sensitive to surface layers (50 μm or so), and not sensitive enough for the determination of many trace and ultratrace element contents. Recently, XRF was used by us for the analysis of several thousands of coins, such as Celtic coins minted from the late 4th century BC to the mid 1st century AD, different mintages of the Roman republic (280–276 BC) [32], denairs of Boleslau II, Duke of Bohemia (972–999 AD), which were historically followed by bracteates (only 150–200 μm thick coins) minted in the period ca. 1220–1300 AD [33], and Hungarian medieval ducats [34]. Coin analyses were aimed at the determination of the purity of the precious metals (Au, Ag) and the presence of additives, and to distinguish between genuine and counterfeit ones (both modern and historical), and also to reveal the way the fake coins were made (amalgamation or plating). Figure 4 shows examples of genuine and fake gold coins analysed. If element detection limits of XRF are insufficient, it is useful to combine

this technique with INAA (when taking the mass of a small specimen is acceptable). This approach was used for the study of Egyptian metal artefacts from Early Dynastic and Old Kingdom periods ca. 3100 BC to 2200 BC, which brought new insights into the provenance of raw materials and archaeometallurgy [35].



Figure 4. Genuine gold Celtic coin (**left**), fake Celtic coin gilded by a thin layer of gold on a copper alloy core (**middle**), and a genuine medieval gold Hungarian ducat (**right**).

3.3. Determination of Matrix of a Bronze Age Bracelet by PAA and Its Age by Radiocarbon Dating

A bracelet made of an organic material from the later Bronze Age with unknown matrix origin was recently found at an ancient fortification in the vicinity of Karlovy Vary (Czech Republic). It was presumed that the matrix was either leather or tree bark, because no other organic material could be considered for ancient decorative objects. Therefore, the nitrogen content was examined, which is significantly different in leather and tree bark, by instrumental PAA (IPAA), and the bracelet age was determined by radiocarbon dating.

IPAA allows non-destructive nitrogen determination, based on the nuclear reaction $^{14}N(\gamma,n)^{13}N$ with half-life $T_{1/2}$ = 9.97 m. The ^{13}N radionuclide is a pure β^+ emitter and the measurement of its non-specific annihilation γ-rays of 511.0 keV is interfered with by other positron emitters, such as ^{11}C ($T_{1/2}$ = 20.4 m), ^{15}O ($T_{1/2}$ = 2.04 m), and ^{18}F ($T_{1/2}$ = 1.83 h). Therefore, irradiation and measurement conditions had to be optimized to eliminate the interference, as described in [11].

For radiocarbon dating, several milligrams of the bracelet were repeatedly leached in 4% HCl, then in 4% NaOH and finally in 4% HCl. The dry pretreated sample was combusted at 900° C and the resulting CO_2 was purified and transferred into a graphitization reactor. The graphitized sample was analysed by AMS at the ATOMKI HAS cooperating laboratory in Debrecen [11].

The absence of bias in the IPAA procedure was tested by the analysis of NIST RM 8433 Corn Bran prepared for irradiation and γ-ray counting in a shape that matched the analysed bracelet specimen as much as possible. The achieved results of the nitrogen determination, 0.893% ± 0.024%, agreed with the NIST reference value of 0.882% ± 0.027% within uncertainty margins, thus validating the procedure used. The validated procedure of nitrogen determination in the bracelet and presumed matrix materials, i.e., cherry tree bark and industrially processed leather, yielded the values given in Table 1.

Table 1. Instrumental photon activation analysis (IPAA) results of total nitrogen (according to [11]).

Sample	Total Nitrogen, wt% [a]
Tree bark	0.74 ± 0.02
Leather	14.17 ± 0.17
Bracelet	0.45 ± 0.02

[a]—value ± expanded uncertainty (coverage factor, k = 2).

The low nitrogen value suggests that the bracelet was made of tree bark. The results of radiocarbon dating yielded the conventional radiocarbon age of the bark bracelet to be 3070 ± 24 years BP (Before Present), which corresponds to the calibrated age of

1408–1266 years BC (probability *p*-value of 95%). The bracelet found at the bottom of the fortification appeared older than the wood (charcoal samples were also analysed) used for the construction of the fortification, which indicates the pre-fortification human exploration of the place [11].

3.4. Radiocarbon Dating of Charcoal Drawings in Kateřinská Cave of the Moravian Karst by AMS

Human activities can be traced in European caves, especially if there are preserved drawings or markings. Here, the results of the radiocarbon dating of charcoal drawings in Kateřinská cave of the Moravian Karst, Czech Republic, by AMS, are reported which are considerably older than previously known Czech Eneolithic drawings in Býčí Skála of the same karst, which were dated for the period spanning from 2885 BC to 3630 BC [26].

In this study, a new wipe-sampling method was developed using quartz wool pre-treated and soaked in dilute HCl, which mostly preserves the graffiti contours (Figure 5) and provides a sufficient mass of charcoal for analysis. The swabs were leached repeatedly in 0.5 M HCl, 0.1 M NaOH, demineralized water and finally with 0.01 M HCl. The subsequent sample processing and data interpretation were analogical to those for other samples, as described in Section 2.5. The ^{14}C analysis results of the graffiti in Kateřinská Cave yielded dates that correspond to the same periods dated using the ceramics found at the cave entrance. Of the several graffities dated employing ^{14}C analysis, the one found in the Main Dome, called "Brain" (Figure 5), appeared to be the oldest, with a calibrated age of 5218–5031 BC.

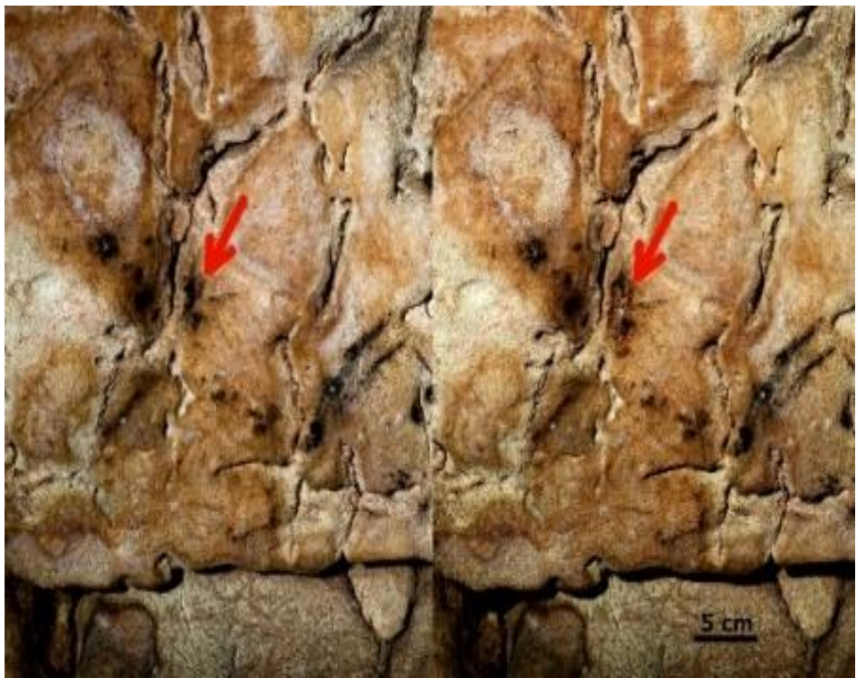

Figure 5. Sampling of "Brain" charcoal graffiti prior to sampling (**left**) and after sampling (**right**).

Thus, it represents the oldest known cave charcoal drawing on the Czech and Moravian territory from the Early Neolithic period [26].

3.5. Assay of Tycho Brahe's Remains by INAA, RNAA and IBA—Was He Poisoned with Hg?

The world-renowned Danish astronomer Tycho Brahe, Imperial astronomer to Emperor Rudolf II, died in Prague in 1601 after a short, 11-day illness after he had attended a banquet at the count of Rosenberg. He drank wine there a little overgenerously without leaving the table due to the etiquette of a nobleman. After his return home, he could not urinate anymore and died with symptoms of uraemia, as described in two contemporary accounts of his illness and death. The third account gave rise to a legend, highly unlikely,

that Brahe died because his bladder burst [36]. Several conspiracy theories regarding Brahe's death have been aired, mostly presuming mercury poisoning. In 2010, Brahe's grave in Prague was reopened by a Czech–Danish consortium and samples of his hair and bones were procured for assay mostly by INAA, radiochemical NAA (RNAA) and IBA.

The cleaned hair samples, about 2 cm long, with identified bulbs were cut into ~5 mm-long sections, and about 20–30 sectioned hair samples weighing 200–300 μg were sealed in pre-cleaned quartz vials (Suprasil® AN, Heraeus), and irradiated at a neutron flux of $3{\cdot}10^{13}$ cm^{-2} s^{-1} in the LVR-15 experimental reactor for 20 h together with blank ampoules, neutron fluence monitors, calibrators and NIST SRM® 1515 Apple Leaves quality control samples in each irradiation batch. The irradiated samples were decomposed and their multi-elemental assay was first performed by INAA, prior to RNAA, to determine Hg, as described previously elsewhere [37]. Lead was determined in two single hairs by μ-PIXE using a Tandetron 4130 MC accelerator with a 2.6 MeV proton beam, focused to a diameter of 1.5 μm by performing multiple scans over 500 μm sections of hair at several distances from the hair bulb using a 0.1 nA beam current for 1–3 h. Bones were mechanically cleaned and their samples with a mass of ~500 mg were pulverized using an agate ball-mill Pulverisette 5 (Fritsch) and assayed by INAA.

The hair samples analysed reflect the intake (exposure) of Hg and other metals over the approximately 2 months prior to Brahe's death, considering the most frequently cited hair growth of 10 mm per month. The time course of Hg values in three samples of Brahe's hair is depicted in Figure 6 and compared with median (solid line) and upper and lower ranges (dashed lines) for the contemporary, unexposed population. It can be seen that for most segments of Brahe's hair, the Hg values are comparable to those for modern populations, although two values slightly exceed the upper range. However, the slight overrun has no toxicological significance, because in cases of moderate intoxication, Hg values in the range of 200 to 800 μg g^{-1} are usually found. The data prove that Brahe was not exposed to (given) lethal doses of Hg during the weeks prior to his death. Similar concentration time trends were found for the elements Fe, As, Ag and Au, with the initial values exceeding those of the present population and decreasing towards Brahe's death. However, no such trend was observed for the elements Cr, Zn, Br, Sb, and Pb [38]. The data concerning the normal and constant levels of Pb in Brahe's hair (Figure 7) are somewhat surprising, because Brahe was not only a famous astronomer, but also an alchemist, and alchemists were frequently exposed to toxic levels of Pb from their experiments. For instance, Sir Isaac Newton, a mathematician, physicist, astronomer, alchemist and theologian, widely recognized as one of the greatest mathematicians and physicists of all time, and considered to be among the most influential scientists, was exposed to Pb and several other toxic elements from his alchemical activities to such an extent that his health collapsed for several years [38].

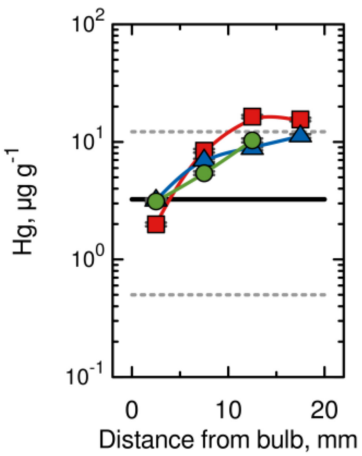

Figure 6. Hg content in three samples of Brahe's hair (distinguished by different symbols), 10 mm of hair represents approximately 1 month of life (modified from [37]).

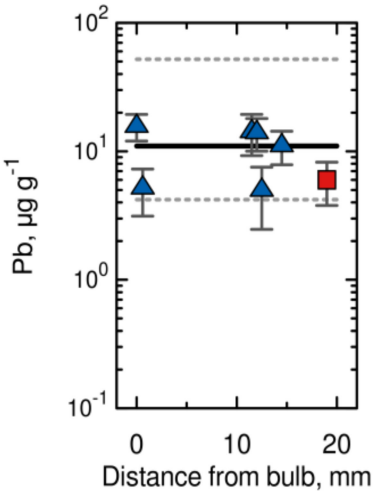

Figure 7. Pb content in two samples of Brahe's hair distinguished by different symbols, 10 mm of hair represents approximately 1 month of life (modified from [37]).

The element concentrations in the bone samples provide information about much longer exposure to these elements compared with hair samples. Slightly elevated concentrations are found only for Co and Au, not for Hg. Thus, Brahe's long-term exposure to Hg can also be excluded.

Another interesting discovery was found following the INAA assay of tiny pieces of discoloured small bones in the nasal opening (*Apertura piriformis*) of Brahe's facial remains (Figure 8). Highly elevated concentrations of Cu and Zn (7780 $\pm$ 307 μg g^{-1} and 8070 $\pm$ 309 μg g^{-1}, respectively) are found. This result seems to elucidate the composition of a shiny nose prosthesis, which Brahe used to wear for many years after he had lost a part of his nose in a duel, and which has never been found in Brahe's tomb. Although it was presumed that the prosthesis was made of Ag or Au, the result (the Cu/Zn ratio) suggests that it was made of brass, which left traces on the nasal bones due to corrosion.



Figure 8. Discoloured bones of Brahe's *Apertura piriformis*.

Recently, there were also attempts to shed more light on Brahe's health status and dietary habits. A palaeopathological assessment provided evidence that Tycho Brahe suffered from diffuse idiopathic skeletal hyperostosis (DISH), and isotope analysis of his skeletal remains, namely the determination of δ^{13}C and δ^{15}N values, showed that the famous astronomer had a rich diet with high protein intake, which resulted in obesity [39]. Radiocarbon dating of cortical femoral tissue samples obtained from Tycho Brahe and his wife Kirsten Barbara Jørgensdatter revealed no reservoir effects, while isotope analysis

provided similar values of $\delta^{13}C$ and $\delta^{15}N$ [40] to those reported by Kacki et al. [39]. The values of $\delta^{13}C$ and $\delta^{15}N$ suggest that the most important protein intake for both Brahe and his wife for many years was freshwater fish from pools with stagnant water [40]. However, these recent studies do not allow a definite diagnosis to be reached and do not reveal straightforwardly a reason for the sudden illness and premature death of the famous astronomer.

4. Conclusions

The unique arsenal of nuclear analytical techniques available at Nuclear Physics Institute (NPI), Řež, employing ion, neutron and photon beams proved very useful, and in some cases even indispensable, for cultural heritage investigations. Either the individual techniques or their combinations were used, as described in Section 3.2, Section 3.3, and Section 3.5, for analyses, which could not be accomplished by other analytical means. The studies performed demonstrate how nuclear physics can contribute to the characterization and identification of cultural heritage objects. We plan the continuation of all of the activities described in this paper, and especially those employing accelerator mass spectroscopy (AMS). This is because NPI has recently acquired a new AMS system MILEA, capable of the determination of very low levels of the cosmogenic radionuclides ^{10}Be, ^{14}C, and ^{26}Al, as well as actinoids (namely isotopes of uranium and plutonium) and selected fission products, such as ^{129}I [18]. Thus, it can be expected that NPI activities in cultural heritage investigations will become increasingly focused on the use of AMS for radiocarbon dating and also on dating with ^{10}Be and ^{26}Al cosmogenic radionuclides, by taking advantage of the excellent parameters and sufficient capacity of the new NPI MILEA AMS system.

Notably, the arsenal of nuclear analytical techniques available at NPI has found many applications in several fields of science and technology other than cultural heritage investigations, namely in material research, environmental control and monitoring, geo- and cosmochemistry, agriculture and nutritional research, and in quality control and reference material preparation, as has been reviewed in several papers [13,41–43]. These activities are planned to continue along with those concerning cultural heritage investigations.

Author Contributions: Conceptualization and writing—original draft preparation, J.K. (Jan Kučera); methodology, validation, investigation, and writing—review and editing, J.K. (Jan Kučera), J.K. (Jan Kameník), V.H., I.K., I.S., K.P.B., M.F. and D.C. All authors have read and agreed to the published version of the manuscript.

Funding: This research was funded by the Ministry of Education, Youth and Sports of the Czech Republic, project No. CZ.02.1.01/0.0/0.0/16_019/0000728.

Data Availability Statement: The data used can be found in the cited publications or can be made available from the authors of the publications upon request.

Conflicts of Interest: The authors declare no conflict of interest.

References

1. Macková, A.; MacGregor, D.; Azaiez, F.; Nyberg, J.; Piasetzky, E. *Nuclear Physics for Cultural Heritage, A Topical Review*; Nuclear Physics Division of the European Physical Society: Mulhouse, France, 2016. [CrossRef]
2. Macková, A.; Kučera, J.; Kameník, J.; Havránek, V.; Šmit, Ž.; Giuntini, L.; Kasztovszky, Z. Nuclear physics for cultural heritage. *Nuovo Cim. C* **2019**, *42*, 53. [CrossRef]
3. Adriaens, M.; Dowsett, M. (Eds.) *Spectroscopy, Diffraction and Tomography in Art and Heritage Science*; Elsevier: Amsterdam, The Netherlands, 2021. [CrossRef]
4. Jeynes, C.; Colaux, J.L. Thin film depth profiling by ion beam analysis. *Analyst* **2016**, *141*, 5944–5985. [CrossRef] [PubMed]
5. Research Reactor LVR-15. Available online: http://reaktory.cvrez.cz/en/research-reactor-lvr-15/ (accessed on 22 January 2021).
6. Řanda, Z.; Frána, J.; Mizera, J.; Kučera, J.; Novák, J.K.; Ulrych, J.; Belov, A.G.; Maslov, O.D. Instrumental neutron and photon activation analysis in the geochemical study of phonolytic and trachytic rocks. *Geostand. Geoanal. Res.* **2007**, *31*, 275–283. [CrossRef]
7. Kubešová, M.; Kučera, J. Validation of k_0 standardization method in neutron activation analysis—The use of Kayzero for Windows programme at the Nuclear Physics Institute, Řež. *Nucl. Instrum. Meth. Phys. Res. A* **2010**, *622*, 403–406. [CrossRef]

8. Kubešová, M.; Kučera, J.; Fikrle, M. A new monitor set for the determination of neutron flux parameters in short-time k_0-NAA. *Nucl. Instrum. Meth. Phys. Res. A* **2011**, *656*, 61–64. [CrossRef]
9. Kubešová, M.; Krausová, I.; Kučera, J. Verification of k_0-NAA results at the LVR-15 reactor in Řež with the use of Au + Mo + Rb (+Zn) monitor set. *J. Radioanal. Nucl. Chem.* **2014**, *300*, 473–480. [CrossRef]
10. Krist, P.; Horák, Z.; Mizera, J.; Chvátil, D.; Vognar, M.; Řanda, Z. Innovations at the MT 25 microtron aimed at applications in photon activation analysis. *J. Radioanal. Nucl. Chem.* **2015**, *304*, 183–188. [CrossRef]
11. Krausová, I.; Tajer, J.; Světlík, I.; Chvátil, D. Matrix determination of Bronze Age bracelet via nitrogen assay by instrumental photon activation analysis and radiocarbon dating of its exact age. *Nucl. Instrum. Methods Phys. Res. B* **2019**, *448*, 26–30. [CrossRef]
12. Jeynes, C.; Palitsina, V.V.; Kokkoris, C.; Hamilton, A.; Grime, G.W. On the accuracy of Total-IBA. *Nucl. Instrum. Meth. Phys. Res. B* **2020**, *465*, 85–100. [CrossRef]
13. Macková, A.; Malinský, P.; Cutroneo, M.; Havránek, V.; Voseček, V.; Flaks, J.; Semián, V.; Vonka, L.; Zach, V.; Bém, P.; et al. Small accelerators and their applications in the CANAM research infrastructure at the NPI CAS. *Eur. Phys. J. Plus* **2021**, *136*, 558. [CrossRef]
14. Maxwell, J.A.; Campbell, J.L.; Teesdale, W.J. The Guelph PIXE software package. *Nucl. Instrum. Meth. Phys. Res. B* **1989**, *43*, 218–230. [CrossRef]
15. Campbell, J.L.; Cureatz, D.J.T.; Flannigan, E.L.; Heirwegh, C.; Maxwell, J.; Russell, J.; Taylor, S. The Guelph PIXE software package, V. *Nucl. Instrum. Meth. Phys. Res. B* **2021**, *499*, 77–88. [CrossRef]
16. Grime, G.W. The 'Q factor' method: Quantitative microPIXE analysis using RBS normalisation. *Nucl. Instrum. Meth. Phys. Res. B* **1996**, *109*, 170–174. [CrossRef]
17. Hajdas, I.; Ascough, P.; Garnett, M.H.; Fallon, S.J.; Pearson, C.L.; Quarta, G.; Spalding, K.L.; Yamaguchi, H.; Yoneda, M. Radiocarbon dating. *Nat. Rev. Methods Primers* **2021**, *1*, 62. [CrossRef]
18. Kučera, J.; Maxeiner, S.; Müller, A.; Němec, M.; John, J.; Světlík, I.; Kameník, J.; Dreslerová, D.; Pachnerová Brabcová, K.; Tecl, J.; et al. A new AMS facility MILEA at the Nuclear Physics Institute in Řež. In Proceedings of the 15th International Conference on Accelerator Mass Spectrometry, ANSTO, Sydney, NSW, Australia, 15–19 November 2021; Available online: https://www.ams15sydney.com/program/PosterT7.01 (accessed on 16 January 2022).
19. Radiocarbon Competence Center. Available online: https://www.atomki.hu/osztalyok/21/bemutatkozas (accessed on 22 January 2022).
20. Synal, H.-A.; Stocker, M.; Suter, M. MICADAS: A new compact radiocarbon AMS system. *Nucl. Instrum. Meth. Phys. Res. B* **2007**, *259*, 7–13. [CrossRef]
21. Longin, R. New method of collagen extraction for radiocarbon dating. *Nature* **1971**, *230*, 241–242. [CrossRef] [PubMed]
22. Gupta, S.K.; Polach, H.A. *Radiocarbon Dating Practices at ANU*; The Australian National University: Canberra, ACT, Australia, 1985.
23. Orsovszki, G.; Rinyu, L. Flame-sealed tube graphitization using zinc as the sole reduction agent: Precision improvement of Environ MICADAS ^{14}C measurements on graphite targets. *Radiocarbon* **2015**, *57*, 979–990. [CrossRef]
24. Handlos, P.; Světlík, I.; Horáčková, L.; Fejgl, M.; Kotik, L.; Brychová, V.; Megisová, N.; Marecová, K. Bomb peak: Radiocarbon dating of skeletal remains in routine forensic medical practice. *Radiocarbon* **2018**, *60*, 1017–1028. [CrossRef]
25. Reimer, P.; Austin, W.; Bard, E.; Bayliss, A.; Blackwell, P.G.; Ramsey, C.B.; Butzin, M.; Cheng, H.; Edwards, R.L.; Friedrich, M.; et al. The IntCal20 Nothern Hemisphere radiocarbon age calibration curve (0–55 cal kBP). *Radiocarbon* **2020**, *62*, 725–757. [CrossRef]
26. Golec, M.; Zajíček, P.; Světlík, I.; Pachnerová Brabcová, K.; Maříkova, L.; Čermáková, E.; Ovsonkova, Z.A. Prehistoric charcoal graffiti discovered in Kateřinská cave, Czech Republic. *Radiocarbon* **2021**, *63*, 473–480. [CrossRef]
27. Andre, M.F. Sandstone weathering rates at the Angkor Temples (Cambodia). In *Heritage, Weathering and Conservation*; Fort, R., Alvarez De Buergo, M., Gomez-Heras, M., Vasquez-Calvo, C., Eds.; Taylor & Francis Group: London, UK, 2006; Volume 1, pp. 165–175.
28. Uchida, E.; Cunin, O.; Suda, C.; Ueno, A.; Nakagawa, T. Consideration on the construction process and the sandstone quarries during the Angkor period based on the magnetic susceptibility. *J. Archaeol. Sci.* **2007**, *34*, 924–935. [CrossRef]
29. Uchida, E.; Watanabe, R.; Cheng, R.; Nakamura, Y.; Takeyama, T. Non-destructive in-situ classification of sandstones used in the Angkor monuments of Cambodia using a portable X-ray fluorescence analyzer and magnetic susceptibility meter. *J. Archaeol. Sci. Rep.* **2021**, *39*, 103137. [CrossRef]
30. Kučera, J.; Novák, J.K.; Kranda, K.; Poncar, J.; Krausová, I.; Soukal, L.; Cunin, O.; Lang, M. INAA and petrological study of sandstones from the Angkor monuments. *J. Radioanal. Nucl. Chem.* **2008**, *278*, 299–306. [CrossRef]
31. Řanda, Z.; Kučera, J.; Soukal, L. Elemental characterization of the new Czech meteorite Morávka by neutron and photon activation analysis. *J. Radioanal. Nucl. Chem.* **2003**, *257*, 275–283. [CrossRef]
32. Vacínová, L.; Militký, J.; Fikrle, M. *Coins of the Roman Republic*; Národní Muzeum: Prague, Czech Republic, 2018.
33. Schneider, P.; Militký, J.; Zaoral, R.; Fikrle, M. *Levínská Olešnice: Nález Mincí ze 13. Století*; Národní Muzeum: Prague, Czech Republic, 2018.
34. Budaj, M.; Polanský, L.; Fikrle, M.; Kriz, E. *Uherské Středověké Dukáty ze Sbírky Národního Muzea*; Národní Muzeum and Abalon: Prague, Czech Republic, 2020.
35. Kmošek, J.; Odler, M.; Fikrle, M.; Korchegina, Y.V. Invisible connections. Early dynastic and old Kingdom Egyptian metalwork in the Egyptian Museum of Leipzig University. *J. Archaeol. Sci.* **2018**, *96*, 191–207. [CrossRef]

36. Rasmussen, K.L.; Kučera, J.; Skytte, L.; Kameník, J.; Havránek, V.; Smolík, J.; Velemínský, P.; Lynnerup, N.; Brůžek, J.; Vellev, J. Was he murdered or was he not? Part I: Analyses of mercury in the remains of Tycho Brahe. *Archaeometry* **2013**, *55*, 1187–1195. [CrossRef]
37. Kučera, J.; Rasmussen, K.L.; Kameník, J.; Kameník, J.; Kubešová, M.; Skytte, L.; Povýšil, C.; Havránek, V.; Velemínský, P.; Lynnerup, N.; et al. Was he murdered or was he not?—Part II. Multielemental analyses of hair and bone samples from Tycho Brahe and histopathology of his bones. *Archaeometry* **2017**, *59*, 918–933. [CrossRef]
38. Spargo, P.E.; Pounds, C.A. Newton´s ´Derangements of his intellect´: New light on an old problem. *Notes Rec. R. Soc. Lond.* **1979**, *34*, 11–32. [CrossRef]
39. Kacki, S.; Velemínský, P.; Lynnerup, N.; Kaupová, S.; Jeanson, A.L.; Povýšil, C.; Horák, M.; Kučera, J.; Rasmussen, K.L.; Podliska, J.; et al. Rich table but short life: Diffuse idiopathic skeletal hyperostosis in Danish astronomer Tycho Brahe (1546–1601) and its possible consequences. *PLoS ONE* **2018**, *13*, e0195920. [CrossRef]
40. Van der Plicht, J.; Drtikolová Kaupová, S.; Velemínský, P.; Smolík, J.; Kučera, J.; Kameník, J.; Havránek, V.; Brůžek, J.; Vellev, J.; Rasmussen, K.L. On the diet of Tycho Brahe and his wife: Did they consume fish from stagnant pools? *Herit. Sci.* **2020**, *8*, 73. [CrossRef]
41. Kučera, J. Laboratory of neutron activation analysis at the Nuclear Physics Institute of the ASCR, Řež. *Nucl. Phys. News* **2011**, *21*, 30–35. [CrossRef]
42. Hnatowicz, V.; Vacík, J.; Macková, A.; Kučera, J. Laboratory for materials analysis by nuclear analytical techniques. *Nucl. Phys. News* **2016**, *26*, 21–26. [CrossRef]
43. Kučera, J. Activation analysis in Czechoslovakia and in the Czech Republic: More than 50 years of activities. *J. Radioanal. Nucl. Chem.* **2018**, *318*, 1473–1492. [CrossRef]